Geosci. Instrum. Method. Data Syst. Discuss., https://doi.org/10.5194/gi-2017-27
Manuscript under review for journal Geosci. Instrum. Method. Data Syst.
Discussion started: 7 June 2017

Geoscientific Instrumentation Methods and Data Systems Discussions

Geoelectric monitoring at the Boulder magnetic observatory

Cletus C. Blum[1], Timothy C. White[1], Edward A. Sauter[1], Duff C. Stewart[1], Paul A. Bedrosian[2], Jeffrey J. Love[1]

[1]U.S. Geological Survey, Geomagnetism Program,
Box 25046 MS 966 DFC, Denver, Colorado 80225, USA

[2]U.S. Geological Survey, Crustal Geophysics and Geochemistry Science Center
Box 25046 MS 964 DFC, Denver, Colorado 80225, USA

Abstract

Despite its importance to a range of applied and fundamental studies, and obvious parallels to a robust network of magnetic-field observatories, long-term geoelectric field monitoring is rarely carried out. The installation of a new geoelectric monitoring system at the Boulder Magnetic observatory of the U.S. Geological Survey is summarized. Data from the system are expected, among other things, to be used for testing and validating algorithms for mapping North American geoelectric fields. An example time series of recorded electric and magnetic fields during a modest magnetic storm is presented. Based upon our experience, we additionally present operational aspects of a successful geoelectric field monitoring system.

Introduction

Geoelectric fields are induced in the Earth's electrically conducting interior by time-dependent geomagnetic field variation sustained by dynamic processes operating in the ionosphere and magnetosphere. This induction occurs all the time, during both magnetically calm and stormy conditions. During intense storms, induced geoelectric fields can drive quasi-direct currents in bulk electric-power grids of sufficient strength to interfere with their operation, sometimes even causing blackouts and damaging transformers [e.g. Boteler et al., 1998; Piccinelli and Krausmann, 2014]. Notably, the magnetic storm of March 1989 [e.g. Allen et al., 1989] caused the collapse of the Hydro-Québec power-grid system in Canada, leaving 6 million people without electricity [Bolduc, 2002; Béland and Small, 2005]. More recently, the Halloween storm of October 2003 caused operational failures in parts of the Swedish power-grid system [Pulkkinen et al., 2005]. Some scenario analyses anticipate that the future occurrence of a rare but extremely intense magnetic superstorm could cause widespread and long-lasting loss of electric-power [e.g. Kappenman 2012] and entail substantial economic cost [e.g. Baker et al., 2008].

In support of a project for modeling and evaluating geoelectric hazards [e.g. Thomson, 2007; Love et al. 2014], in June of 2016, the Geomagnetism Program of the U.S. Geological Survey (USGS) commenced long-term geoelectric field monitoring at its Boulder, Colorado magnetic observatory. The Boulder geoelectric monitoring project partially fulfills a directive in the United

Geosci. Instrum. Method. Data Syst. Discuss., https://doi.org/10.5194/gi-2017-27
Manuscript under review for journal Geosci. Instrum. Method. Data Syst.
Discussion started: 7 June 2017

Geoscientific Instrumentation Methods and Data Systems Discussions
Open Access
EGU

States National Space Weather Action Plan [NSTC, 2015, Goal 5.5.4] (one of many given to different agencies) for the Department of Interior to "assess and pilot a geoelectric monitoring capability." It is further consistent with strategic goals of the USGS Hazard Mission for enhancing observations, pursuing fundamental understanding, and improving hazard assessments [Holmes et al. 2013, Goal 1]. Geoelectric field monitoring is a natural extension of the geomagnetic monitoring that is already the responsibility of the USGS Geomagnetism Program [Love & Finn, 2011], and it is similar to long-term geoelectric monitoring projects supported in other countries, including Great Britain [Kelly et al., 2013] and Japan [Fujii et al., 2015] and to shorter-term campaign-style measurements common to magnetotelluric surveys [e.g. Ferguson, 2012]. From 1932 to 1942, analog geoelectric measurements were supported at the Tucson magnetic observatory [Rooney, 1949]; from 1988 to 1995, geoelectric monitoring was performed in Parkfield California as a part of an earthquake research project [Park, 1997]; otherwise, there has been very little multi-year geoelectric monitoring carried out in the United.

The Boulder site

The Boulder magnetic observatory facility [Love et. al., 2015] is located on a flat-top butte, north of the city of Boulder, Colorado, and east of the United States Rocky Mountains. The land is rocky and sandy, sparsely covered with grass and cacti. The climate is semi-arid; summers are hot (>30° C is common) with occasional thunderstorms; winters are cold (often <-5° C) with occasional snowfall. The Boulder observatory is one of 14 supported by the USGS Geomagnetism Program, and it is part of the International Real-time Magnetic Observatory Network [www.intermagnet.org, Love and Chulliat 2013]. The observatory is also used by Geomagnetism Program engineers and technical staff to develop and test new sensors, acquisition systems, and operational procedures. The geoelectric monitoring system described herein are located southwest of the observatory's office building and primary geomagnetic monitoring systems; see Figure 1.

Electrodes and their installation

Geoelectric data are obtained by measuring the voltage between pairs of non-polarizable electrodes over time. For geoelectric monitoring at Boulder, Borin Stelth® 2 Silver-Silver Chloride (Ag-AgCl) electrodes were selected for their thermal stability, low noise characteristics, long expected service life (>30 years), and relatively large surface area (200 cm^2); see Figure 2. Electrode noise levels have been estimated to be significantly less than 1 mV based upon long-term measurements of electrode potential in a temperature and salinity-controlled tank. In June of 2016, six electrodes were installed: two located near the data acquisition system, and one each located 100 and 200 meters to the west and south from there. The electrodes were buried to reduce grounding changes caused by time variation in soil moisture content and temperature that can impart unwanted types of voltage variation. As shown schematically in Figure 3, at each electrode location, a 1-m deep hole was dug; this was then partially filled with a thick layer of bentonite clay, a substance that is very absorbant and commonly used as a ground-water barrier. A 20-cm diameter, 1.25-m long, open-ended, polyvinyl chloride (PVC) pipe was placed vertically in the hole and in contact with the bentonite; an electrode was placed in the bottom of the tube

with connecting wires leading out the top end. The tube was then partially filled with additional bentonite until the electrode was covered; the rest of the tube was backfilled with sand; the space around the outside PVC tube was filled with native rock and sand. The electrodes are connected to the acquisition system using shielded coaxial cables further protected by PVC conduit. Two electrodes are located near the acquisition system; one is used for the 100-m dipoles and the other is used for 200-m dipoles; additional empty PVC pipes were installed in parallel for possible future electrode emplacement that might be needed for testing and to provide redundancy. Contact resistances between each pair of electrodes range from 200-300 Ω.

Data acquisition and management

Electrode voltage measurements are acquired using the Observation Reconfigurable Input and Output System (ObsRIO) that USGS engineers developed in-house using the CompactRIO (cRIO) hardware platform manufactured by National Instruments Corporation; the system is solar powered; see Figure 4. The two standard data types acquired by ObsRIO are discrete 10 Hz values and discrete 1-sec values. Ten hertz data values are formed from 100 Hz analog- and digitally-filtered data, and the 1 second values are formed from the 10 Hz values. This data construction process effectively eliminates aliasing from geoelectric variation with periods of less than 0.1-sec (frequencies greater 10 Hz), but, otherwise, the 0.1-sec and 1 sec values are not processed in any way. Data from the Boulder ObsRIO systems are transmitted to the USGS database system, EdgeCWB [Patton et al., 2015], in Golden, Colorado via internet protocols in near-real-time. Geomagnetism Program personnel make regular checks of the Boulder geoelectric data to guard against artificial interference and to ensure continuity of operations.

Example data

In Figure 5 we show three days of Boulder geomagnetic and geoelectric data recording a geomagnetic storm that occurred in October 2016. In global terms, the storm attained a maximum Dst = -104 nT; maximum Kp = 6. Local to Boulder, however, the east geomagnetic component saw a very abrupt and high amplitude signal (~150 nT), which induced a large geoelectric signal in the north geoelectric component. The lowest frequency (diurnal) signals observed in the geomagnetic time series are not reproduced in the geoelectric data due to a 30,000 second high-pass analog filter within the acquisition system. All the measured geoelectric field variation is well correlated with geomagnetic variation and is consistent with induction in the solid-earth. Note, furthermore, that the consistency between the geoelectric time series for the 100 and 200-m dipoles.

Using the data

A high priority for monitoring and assessing geoelectric hazards is the development of capabilities for making maps of the geoelectric field, especially in real-time [e.g. NSTC, 2015, Action 5.5.6]. One approach to regional and continental-scale geoelectric field mapping is convolving maps of Earth impedance with maps of geomagnetic activity [e.g. Thomson, 2007; Love et al. 2014]. Toward this end, long-term surface geoelectric field data, spanning both quiet

and storm times, are critical to validating predicted field data and to benchmarking different modeling approaches [e.g. Kelbert et al. 2017; Bonner and Schultz 2017]. Additionally, surface impedance functions can be calculated from synchronous electric and magnetic time series, as is commonly done with magnetotelluric survey data. Long-term (months to years) geoelectric time series data, as described here, constrain estimates of surface impedance to longer periods than traditional magnetotelluric studies, facilitating investigations into deep-earth conductivity structure. Finally, continuous recording of geoelectric and geomagnetic time series data, particularly at sampling frequencies sufficient to capture the magnetotelluric 'dead-band' (10-0.1 Hz), can serve as remote-reference data for regional magnetotelluric surveys [Gamble et al. 1979; Egbert 1997]. The availability of such data in near-real-time can reduce the logistical and cost overhead associated with such surveys and increase data quality.

Operational aspects of long-term electric field monitoring

Long term electric-field monitoring introduces technical challenges that are distinct from traditional magnetotelluric campaign or array deployments. As with other monitoring studies, power supply, telemetry and system reliability are important design considerations for a successful electric-field monitoring system. Furthermore, long-term electrode deployment adds additional critical design elements, including thermal stability, moisture stability and lightning suppression. We describe below aspects of the Boulder installation that we consider important to achieving continuous, stable, low-noise geoelectric field data.

Long-term electric-field measurements are critically dependent upon the use of stable, low-noise non-polarizable electrodes. A variety of electrode chemistries exist, with Ag-AgCl and Pb-$PbCl_2$ being two of the more commonly used types. Both of these electrode types are known for their low noise levels, small thermal coefficients, and long-term stability (Petiau, 2000; Clerc et al., 1998). The earth environment in which the electrodes are placed is additionally important. In particular, greater thermal and moisture stability reduces non-inductive signals (e.g. diurnal signals due to surface temperature variations). Toward this end, the USGS electrodes are buried 1 meter deep. Electrode noise further scales with the contact resistance between the electrode and the earth. To minimize both, the earth within an area of 0.5 m^2 was removed and replaced with an electrically-conductive bentonite slurry. A 1.25-m long, (1.0-m below ground) PVC tube was emplaced into the bentonite to facilitate the installation and, if necessary, replacement of the electrodes. The electrodes were placed into the bentonite slurry, covered with an additional layer of bentonite, and the remainder of the PVC tube was filled with sand. Caps were subsequently installed to seal the tube and prevent loss of moisture. To provide additional reliability and redundancy, a network of electrodes were installed at each location.

The electrodes are connected via coaxial cable to the data acquisition system. Coaxial cable is selected to reduce the introduction of capacitive noise via the long cable length deployed for this application. The cable shields are grounded near the data acquisition system but isolated at the electrode ends to avoid creating ground loops through the shielding. The coaxial cable was further installed in PVC conduit to protect the cables from damage due to wildlife. Strain relief was added to the PVC conduit at 30 meters intervals to prevent damage to the conduit and cable

during seasonal thermal expansion and contraction.

Lightning suppression, attenuation and protection are of the utmost importance in collecting continuous long-term geoelectric field data. On two separate occurrences, buildings at the Boulder Magnetic Observatory (BOU) have been directly struck by lightning. Significant effort must be made to protect recording systems from damage under such conditions. The USGS has installed a significant grounding system at the data acquisition site, consisting of a large steel ground rod driven 2.34 meters deep. The coaxial shields are all connected to this ground, which provides an electrical path for lightning induced signals and other noise sources incident on the shields. The electrodes are further connected to a pre-amplifier and lightning isolation circuit board. The board was originally designed for the NIMS portable MT system, developed by Narod Geophysics, LTD. There are two components of lightning protection integrated on this board. First are a series of 75 V_{DC} spark gap devices, connected individually to each incoming electrode connection. Additionally, varistors are used in a suppression mode to shunt excessive currents incident on the incoming channels. This board has been used to collect hundreds of thousands of hours of data for the EarthScope US Array program with very few cases of failure from lightning.

Amplification and filtering can be an important component of electric-field monitoring depending upon the application as well as the sensitivity and dynamic range of the data acquisition system. Quiet-time electric-field amplitudes are on the order of 0.1mV/km or less; hence measured voltages across electrode pairs separated by ~100 m may be on the order of 0.01 mV. Instrument gain is commonly used to amplify the raw signals; the gain at the Boulder monitoring station is a factor of 10. Filtering may also be beneficial to obtaining quality electric-field data. There are two analog filters incorporated within the Boulder data acquisition system. A notch filter attenuates 60 Hz signal, common to North America's power distribution network, by a factor of at least 20 dB. An additional analog high-pass filter, with a time constant of roughly 10.5 hours, can optionally be turned on. This filter may be used to attenuate long-period signals, including diurnal signal arising from thermal fluctuations in the electrodes and long-term drift.

A low-noise, high input-impedance data acquisition system with moderately high sample rate is needed for geoelectric field monitoring. To meet this need we developed the Observation Reconfigurable Input and Output System (ObsRIO) based on the CompactRIO (cRIO) hardware platform manufactured by National Instruments (NI). A key design aspect of the ObsRIO platform is its modularity and ability to change configurations in response to rapidly changing scientific needs. Minimal development time is required to create new images of ObsRIO for different scientific applications. The USGS has, for example, designed a portable magnetotelluric variant of the system which acquires both electric and magnetic field data and is battery powered.

The ObsRIO employs 4-channel simultaneous sampling on a 24-bit, +/-10 VDC (direct current voltage) analog to digital converter (ADC, NI 9239). The ADC is configured to sample at a frequency of 10 kHz. A box-car filter is used to decimate the data from 10 kHz to 1 kHz and ultimately to separate 100 Hz, 10 Hz, and 1 Hz data output streams for logging and transmission. A GPS clock was used to discipline the FPGA (field programmable gate array) clock, a process

where the GPS signal is used to constantly calibrate the FPGA clock. Timestamped samples are passed into a FIFO for further processing, logging and transmission on the real-time controller for the cRIO chassis. Pairing the ObsRIO system with a cellular device allows for real-time data collection and transmission.

The data acquisition system was finally designed with automated switching power-source control. ObsRIO automatically charges one battery, while powering the system from a separate battery electrically isolated from the charging source. A series of programmable relays and low resolution ADCs are used to set the power supply state for the system and switch charging and load batteries as needed. This is an important aspect of the ObsRIO system, as noisy power sources (such as solar) are kept from contaminating the desired geoelectric fields. This feature is additionally critical to campaign style deployments, which rely upon batteries and solar power for power.

Disclaimer

Any use of trade, firm, or product names is for descriptive purposes only and does not imply endorsement by the U.S. Government.

Acknowledgements

We thank J. McCarthy and J. L. Slate for reading a draft manuscript. Boulder geoelectric field data can be viewed on the USGS geomagnetism plots page (http://geomag.usgs.gov/plots/) and downloaded from (http://dev-geomag.cr.usgs.gov/ws/edge/). We thank T. Theissen from Borin Manufacturing Inc. for providing the electrodes used at the Boulder magnetic observatory.

References

Allen, J., L. Frank, H. Sauer and P. Reiff (1989) Effects of the March 1989 solar activity, Eos Trans. Am. Geophys. Union, 70(46), 1479, 1486-1488, doi:10.1029/89EO00409.

Béland, J. and K. Small (2005) Space weather effects on power transmission systems: The cases of Hydro-Québec and Transpower New Zealand Ltd, in Effects of Space Weather on Technology Infrastructure, edited by Daglis, I. A., pp. 287-299, Springer, Dordrecht, The Netherlands, 10.1007/1-4020-2754-0_15.

Bolduc, L. (2002) GIC observations and studies in the Hydro-Québec power system, J. Atmos. Solar-Terr. Phys., 64(16), 1793-1802, doi:10.1016/S1364-6826(02)00128-1.

Bonner, L R., IV and A. Schultz (2017) Rapid prediction of electric fields associated with geomagnetically induced currents in the presence of three-dimensional ground structure: Projection of remote magnetic observatory data through magnetotelluric impedance tensors, Space Weather, 15(1), 204–227, doi:10.1002/2016SW001535.

Boteler, D. H., R. J. Pirjola and H. Nevanlinna (1998) The effects of geomagnetic disturbances on electrical systems at the Earth's surface, Adv. Space Res., 22(1), 17-27, doi:10.1016/S0273-1177(97)01096-X.

Clerc, G., Petriau, G., and Perrier, F. (1998) The Garchy 1995-1996 electrode experiment technical report, edited by CEA.

Egbert, G.D. (1997) Robust multiple-station magnetotelluric data processing, Geophys. J. Intl., 130, 10.1111/j.1365-246X.1997.tb05663.x.

Ferguson, I. J. (2012) Instrumentation and field procedure, in The Magnetotelluric Method, edited by Chave, A. D. and A. G. Jones, pp. 421–479, Cambridge Univ. Press, Cambridge, UK.

Fujii, I., t. Ookawa, S. Nagamachi and T. Owada (2015) The characteristics of geoelectric fields at Kakioka, Kanoya, and Memambetsu inferred from voltage measurements during 2000 to 2011, Earth Planets Space, 67, 62, doi:10.1186/s40623-015-0241-z.

Gamble, T. D., Goubou, W. D., and Clarke, J. (1979) Magnetotellurics with a remote magnetic reference, Geophysics, 44, 53-68.

Holmes, R. R., et al. (2013) U.S. Geological Survey Natural Hazards Science Strategy -- Promoting the Safety, Security, and Economic Well-Being of the Nation, pp. 1-79, USGS Circular, 1383-F.

Kappenman, J. G. (2012) A perfect storm of planetary proportions, IEEE Spectrum, 49, 26-31.

Kelbert, A., C. Balch, A. Pulkkinen, G. D. Egbert, J. J. Love, E. J. Rigler and I. Fujii (2017) Methodology for time-domain estimation of storm-time electric fields using the 3D Earth impedance, submitted.

Kelly, G., T. Shanahan, C. Beggan, A. Swan, A. Thomson (2013) Early results from the UK geo-electric field monitoring project, The UK National Astronomy Meeting, General MIST Poster Session, P12.5, St. Andrews, July 1-5.

Love, J. J. and C. A. Finn (2011) The USGS Geomagnetism Program and its role in space weather monitoring, Space Weather, 9, S07001, doi:10.1029/2011SW000684.

Love, J. J. and A. Chulliat (2013) An international network of magnetic observatories, Eos Trans. Am. Geophys. Union, 94(42), 373-374, doi:10.1002/2013EO420001.

Love, J. J., E. J. Rigler, A. Pulkkinen and C. C. Balch (2014) Magnetic storms and induction hazards, Eos Trans. Am. Geophys. Union, 95(48), 445-446, doi:10.1002/2014EO480001.

Love, J. J., C. A. Finn, K. L. Pedrie and C. C. Blum (2015) The Boulder magnetic observatory, pp. 1-8, USGS Open-File Report, 2015-1125, doi:10.3133/ofr20151125.

NSTC (2015) National Space Weather Action Plan, pp. 1-38, Executive Office, National Science and Technology Council, Washington, DC.

Park, S. K. (1997) Monitoring resistivity change in Parkfield, California: 1988–1995, J. Geophys. Res., 102(B11), 24545–24559, doi:10.1029/97JB02080.

Patton, J. M., D. C. Ketchum and M. R. Guy (2015) An overview of the National Earthquake Information Center acquisition software system, Edge/Continuous Waveform Buffer, Open-File Report 2015-1174, pp. 1-10, doi:10.3133/ofr20151174.

Petiau, G. (2000) Second generation of lead-lead chloride electrodes for geophysical applications, Pure Appl. Geophy., 157, 357-382.

Piccinelli, R. and E. Krausmann (2014) Space Weather and Power Grids -- A Vulnerability Assessment, pp. 1-53, European Union, Luxembourg.

Pulkkinen, A., S. Lindahl, A. Viljanen and R. Pirjola (2005) Geomagnetic storm of 29-31 October 2003: Geomagnetically induced currents and their relation to problems in the Swedish high-voltage power transmission system, Space Weather, 3(8), S08C03, doi:10.1029/2004SW000,123.

Rooney, W. J. (1949) Earth-Current Results at Tucson Magnetic Observatory, 1932-1942, pp. 1-309, Carnegie Institute, Washington, DC.

Thomson, A. W. P. (2007) Geomagnetic hazards, in Encyclopedia of Geomagnetism and Paleomagnetism, edited by Gubbins, D. and E. Herrero-Bervera, pp. 316-319, Springer, Dordrecht, The Netherlands, doi:10.1007/978-1-4020-4423-6_117.

Figure captions

Figure 1: Map of geoelectric-monitoring deployment at the Boulder observatory. North is up.

Figure 2: The Borin Stelth® electrodes used for geoelectric-monitoring at the Boulder observatory.

Figure 3: Schematic of electrode installation.

Figure 4: Geoelectric field data acquisition system at the Boulder observatory. (a) View to the northeast of the data acquisition system. Electric field lines, protected by PVC conduit, extend west and south. (b) Interior view of data acquisition system in environmentally-sealed enclosures. Electric, and optionally magnetic, inputs are brought into the right enclosure with shielding tied to the observatory grounding system. The left enclosure contains the ObsRIO is in the upper left, the switching power source controller on the right, and a cellular model in the center.

Geosci. Instrum. Method. Data Syst. Discuss., https://doi.org/10.5194/gi-2017-27
Manuscript under review for journal Geosci. Instrum. Method. Data Syst.
Discussion started: 7 June 2017

Geoscientific Instrumentation Methods and Data Systems Discussions
Open Access
EGU

353
354 **Figure 5:** Three days of geomagnetic and geoelectric field variation recorded at the Boulder
355 observatory: (a) north (blue) and east (gray) geomagnetic components, (b) north geoelectric
356 component, 100 (black) and 200 (red) dipole, (c) east geoelectric component, 100 (black) and 200
357 (red) dipole.
358
359
360
361
362
363
364
365
366
367
368
369
370

371
372
373
374 Figure 1.
375
376
377

Geosci. Instrum. Method. Data Syst. Discuss., https://doi.org/10.5194/gi-2017-27
Manuscript under review for journal Geosci. Instrum. Method. Data Syst.
Discussion started: 7 June 2017

Figure 2.

Geosci. Instrum. Method. Data Syst. Discuss., https://doi.org/10.5194/gi-2017-27
Manuscript under review for journal Geosci. Instrum. Method. Data Syst.
Discussion started: 7 June 2017

Geoscientific Instrumentation Methods and Data Systems Discussions
Open Access
EGU

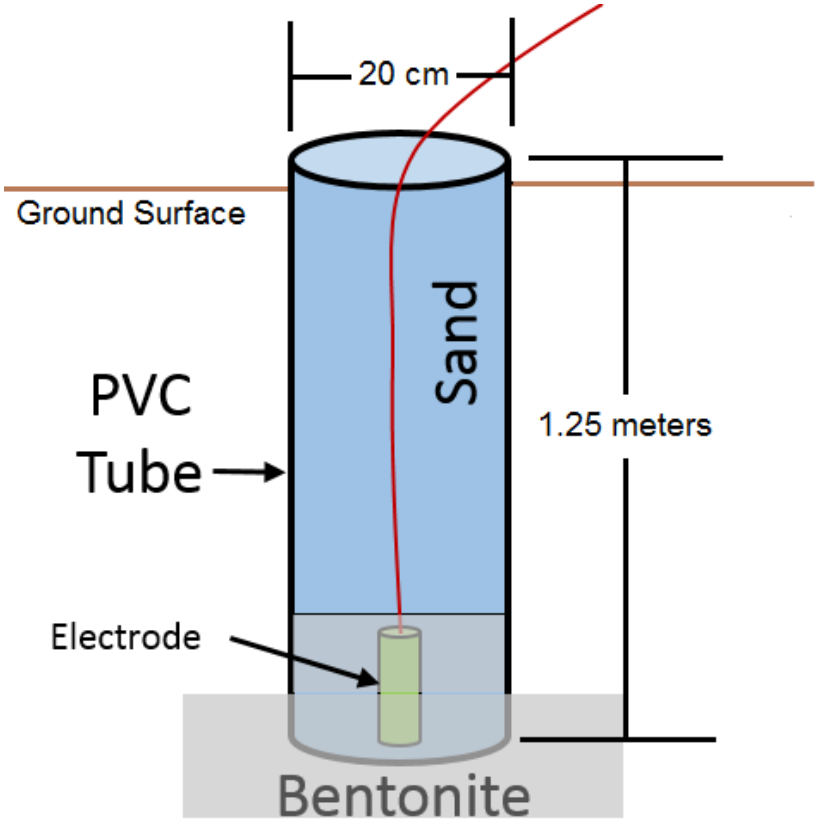

Figure 3.

Geosci. Instrum. Method. Data Syst. Discuss., https://doi.org/10.5194/gi-2017-27
Manuscript under review for journal Geosci. Instrum. Method. Data Syst.
Discussion started: 7 June 2017

Geoscientific Instrumentation Methods and Data Systems Discussions
Open Access
EGU

Figure 4(a)

Geosci. Instrum. Method. Data Syst. Discuss., https://doi.org/10.5194/gi-2017-27
Manuscript under review for journal Geosci. Instrum. Method. Data Syst.
Discussion started: 7 June 2017

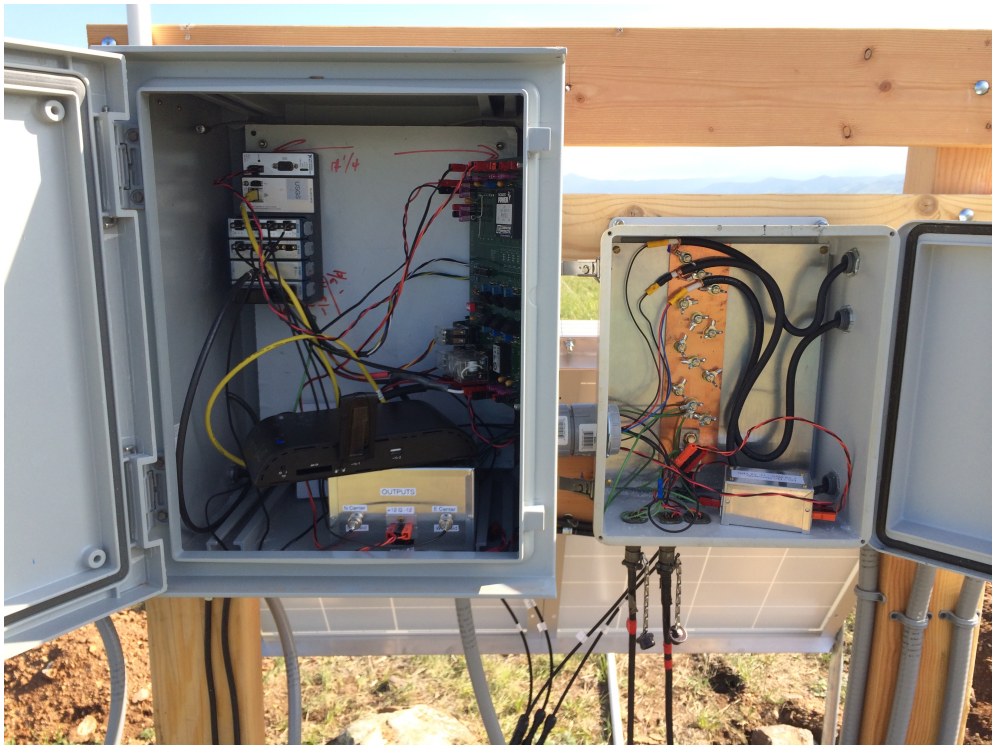

Figure 4(b).

Geosci. Instrum. Method. Data Syst. Discuss., https://doi.org/10.5194/gi-2017-27
Manuscript under review for journal Geosci. Instrum. Method. Data Syst.
Discussion started: 7 June 2017

Geoscientific Instrumentation Methods and Data Systems Discussions

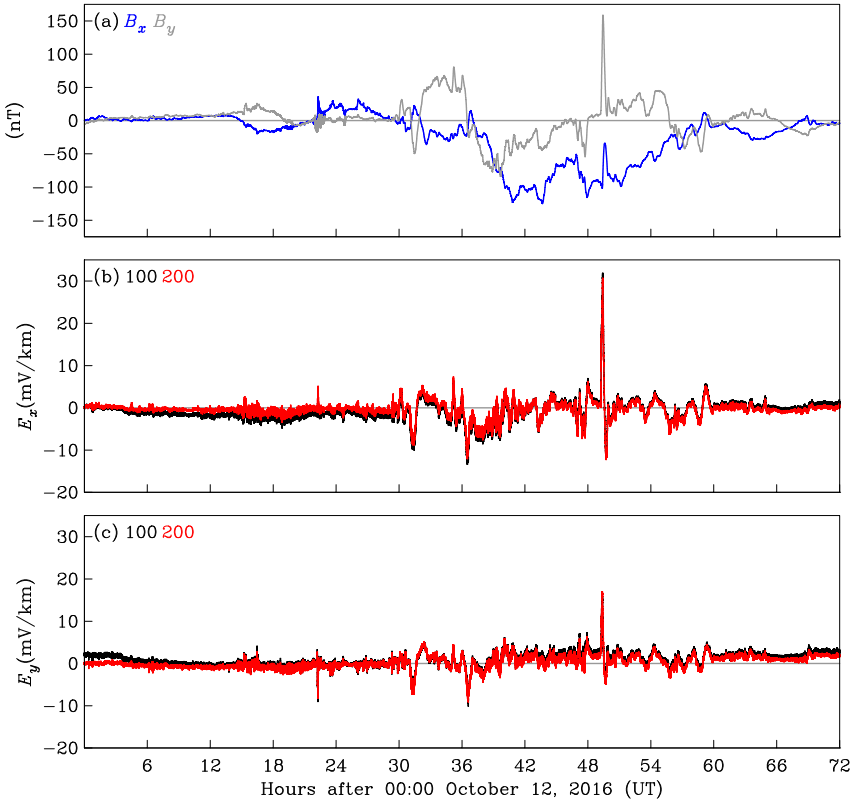

459